



Seismic risk assessment, damage estimation, and strengthening of seismic construction standards in Morocco

Adil Ziraoui¹ · Benaissa Kissi¹ · Hassan Aaya² · Najoua Mrabet³ · Ilhame Azdine¹

Received: 11 March 2024 / Revised: 19 April 2024 / Accepted: 25 April 2024 / Published online: 7 May 2024
© The Author(s), under exclusive licence to Springer Nature Switzerland AG 2024

Abstract

The increasing interest in seismic risk assessment in Morocco is due to the growing frequency of earthquakes, such as the one in Al Haouz in 2023, and the rapid population expansion in these areas. This study focuses on regions with moderate to high seismic activity to better understand the seismic risk in these areas. A critical aspect of this assessment is establishing damage (or fragility) curves, which are necessary for assessing damage levels and making decisions regarding the renovation or demolition of structures. However, a shortfall in seismic regulations is the constant behavior factor, regardless of seismicity level (zones 3, 4, and 5) or structure height. Moroccan seismic regulations (RPS2000) and international standards generally advocate for a fixed value of the behavior factor but often neglect crucial parameters such as structure height and local seismic intensity.

Keywords Seismic zone · Pushover analysis · Over-strength factor · Global ductility · Probability · Fragility curves · RPS 2000

1 Introduction

By its geographical location, Morocco is located on the northwestern edge of the African plate, which is in a continuous movement of approach and collision with the Eurasian plate. Over more than 110 years of macroseismic and instrumental observations, our country has witnessed several devastating earthquakes, among which the 1960 Agadir earthquake ($M_w = 5.9$) remains particularly impactful. This event led to the destruction of over 75% of the city and numerous surrounding villages, resulting in the loss of 12,000 lives. More recently, the earthquake that occurred on the night of Friday, September 8, 2023, with a magnitude of 6.8 on the Richter scale, struck the province of Al-Haouz,

ranking among the most violent in the history of Morocco. The latest assessments report 2,946 deaths, 5,674 injuries, and material damages estimated at nearly 10 billion dollars. Considering these situations, it is imperative to develop effective policies and action plans aimed at mitigating seismic risks in Morocco and enhancing the country's resilience to earthquakes [1–3].

The seismicity of Morocco has been unveiled thanks to the development and extension of the seismological network and the numerous research works and field missions carried out. A delimitation, as precise as possible, of the potentially seismogenic zones and a seismotectonic analysis allowing the determination of the active faults contribute to lead seismic zoning which constitutes an essential step in the evaluation of the seismic hazard. Four main parameters must be taken into account: the location, the date, the magnitude, and the effects that the earthquake can cause on the ground surface. Since predicting earthquakes accurately is currently impossible, long-term forecasting and prevention stand as the only viable methods to mitigate earthquake damage. Therefore, any engineering decisions regarding urban planning, spatial organization, or earthquake preparedness must rely on understanding the characteristics of known and potential earthquakes [4].

✉ Adil Ziraoui
adil_ziraoui@hotmail.com

¹ LISPS2I, National School of Arts and Crafts, Hassan II University, Casablanca, Morocco
² LMSI, International University of Casablanca, Casablanca, Morocco
³ LASTIMI Laboratory Systems Analysis Information Processing and Industrial Management, High School of Technology of Salé, Mohammed V University of Rabat, Rabat, Morocco

Preventive measures have been implemented to mitigate damages caused by earthquakes. The introduction of the national seismic standard R.P.S. in 2000 and its revision in 2011 marked crucial milestones [5, 6]. Additionally, numerous studies have been conducted to assess seismic risk and guide urban planning decisions. The literature proposes several methods to address this issue on a large scale, which can be classified into three distinct categories: i) Empirical Methods: These methods rely on reports of damages caused by earthquakes and building characteristics to estimate a seismic vulnerability index. They were the only reasonable approaches available for analyzing seismic risks on a large scale; ii) Mechanical and Analytical Methods: More detailed but requiring more work, these methods use more complex algorithms to assess vulnerability, allowing for more in-depth and detailed studies; iii) Hybrid Methods: These methods combine the advantages of the two previous approaches. They can be particularly useful when data on damages at certain intensity levels are limited, and they allow for the adjustment of analytical models. Additionally, the use of observational data reduces the computational effort needed to produce a comprehensive set of analytical vulnerability curves [7].

The study of seismic vulnerability of a given seismic movement consists of determining the buildings and structures most vulnerable to the earthquake at the level of a region, a city, or a large number of buildings. A seismic vulnerability study is the first step toward determining the buildings requiring possible reinforcement. Given the complexity of the problem of assessing the seismic vulnerability of existing buildings, a new method has emerged in recent years. This method, known as the capacity spectrum method "ATC 40", has been published in the United States by "Applied Technology Council" and is designed for reinforced concrete constructions. In this method, the level of performance is evaluated in terms of displacements and not in terms of forces, as during deformations the degree of damage varies according to a function of displacements than of forces. ATC 40 is based on the non-linear static "pushover" method. This method can be used for single model structures in the first analysis; it allows a more realistic approach to the behavior of the supporting structures. This method is more demanding and more consequent, and is recommended above all for existing buildings, for which a more favorable evaluation of the seismic safety can avoid expensive reinforcement measures [8].

In this study, we investigate structures located in seismic zones of varying intensities, specifically zones 3, 4, and 5 according to Moroccan seismic regulations, assessing their vulnerability and associated risk for different structures, and calculating the behavior factor. Moroccan seismic regulations (RPS Morocco 2000), like many international

regulatory codes, advocate for a fixed value of the behavior factor R based solely on the nature of the system, without considering several other parameters, although factors such as the seismic zone and the size of the structure are highly significant. This study aims to examine the impact of the seismic zone and the height of the structure on the behavior factor R of reinforced concrete structures. We evaluate behavior factor R by considering the reduction factor Ω , linked to the structure's over-strength, and its deformation capacity in the plastic domain, represented by the reduction factor R_{μ} associated with overall ductility.

2 Seismic hazard

To simplify the calculation of seismic loads and to standardize structural design requirements across large regions of the country, the RPS 2000 version 2011 uses the zone approach. This involves dividing the country into several zones of homogeneous seismicity with approximately the same level of seismic hazard for a given probability of occurrence.

The seismic zone map adopted by the RPS 2000 has five zones related to the maximum horizontal ground acceleration for a 10% probability of occurrence in 50 years. This probability is considered reasonable, as it corresponds to moderate earthquakes likely to occur several times in the life of a structure [5, 6].

In each zone, the parameters defining the seismic hazard, such as horizontal ground acceleration, are considered to be constant with:

$$\text{Zone 1: } A_{\max}/g = 0.04$$

$$\text{Zone 2: } A_{\max}/g = 0.07$$

$$\text{Zone 3: } A_{\max}/g = 0.1$$

$$\text{Zone 4: } A_{\max}/g = 0.14$$

$$\text{Zone 5: } A_{\max}/g = 0.18$$

The map of seismic zones in Morocco is presented in Fig. 1

3 Non-linear static method (pushover analysis)

3.1 Pushover curve

The pushover analysis is a non-linear static analysis conducted under constant gravity loads and monotonically increasing horizontal loads. It can be applied to verify the structural performance of the newly designed or existing building. The capacity curves (pushover curves) obtained

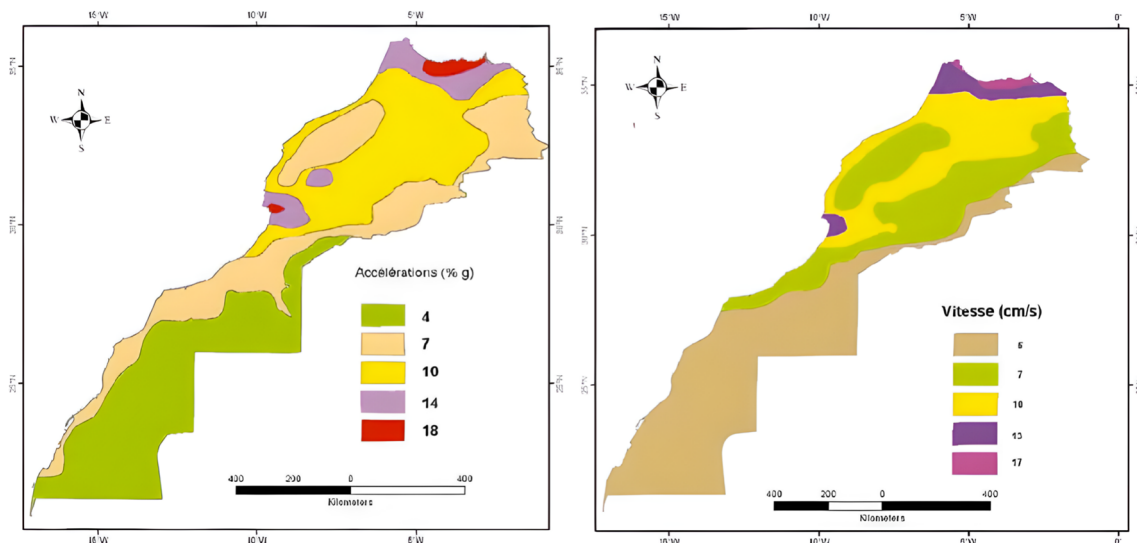


Fig. 1 Map of the five seismic zones of Morocco [6]

give the relationships that exist between the different factors, namely: the behavior factor R , the reduction factor Ω due to the over-strength, and the reduction factor R_μ due to the global ductility of the structure in Fig. 2 [9–12].

3.2 Capacity spectrum and performance point

The capacity spectrum is obtained by two transformations:

The shear force V_b is converted into spectral acceleration S_a , and the actual displacement at the roof U_t is transformed into spectral displacement S_d (Fig. 3) [12]:

$$S_a = \frac{V_b}{M_1} \quad S_b = \frac{u_t}{\Gamma_1 \phi_{t,1}}$$

M_1 is the effective mass of the construction, $\phi_{t,1}$ is the amplitude of the first mode of vibration at the apex, and

Fig. 2 Relationship between behavior factor R , overstrength factor Ω and ductility factor R_μ [12]

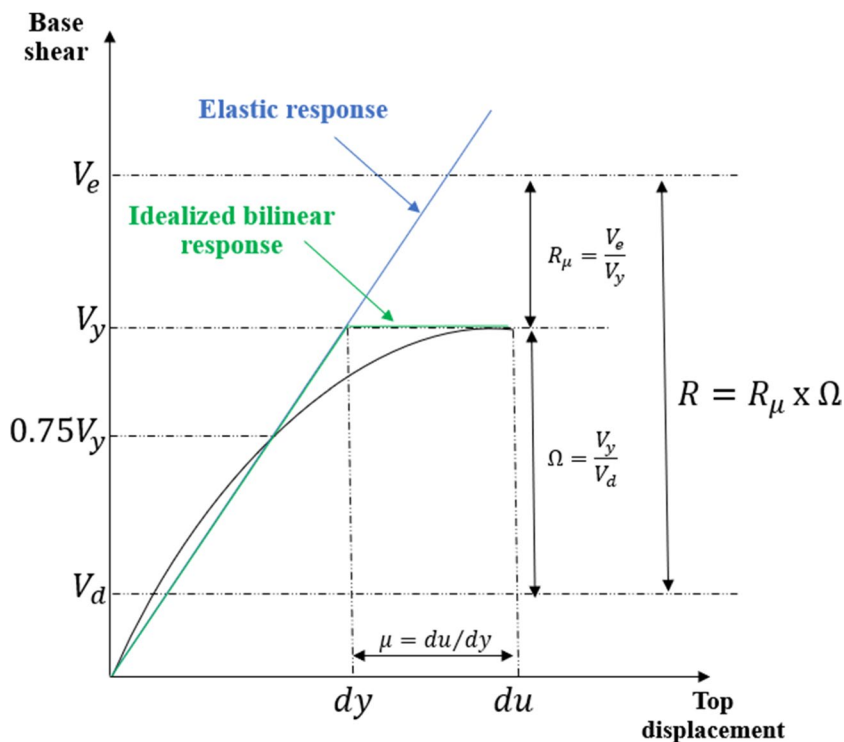
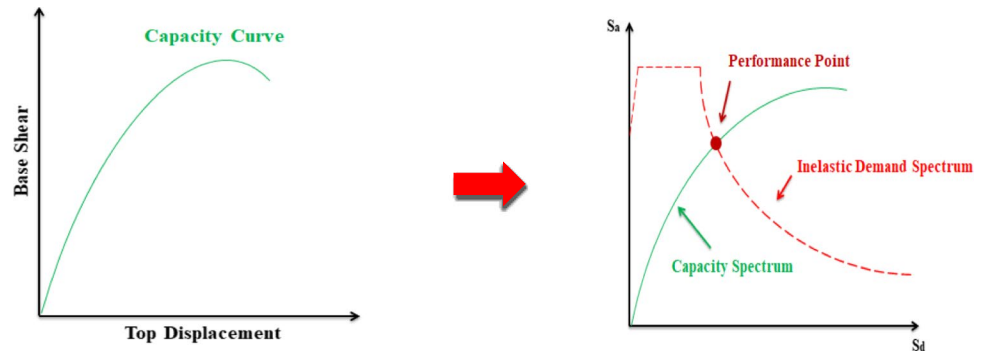


Fig. 3 Capacity and demand [12]



Γ_1 is the modal participation factor corresponding to the first vibration mode.

4 Methods for assessing the ductility factor R_μ

The assessment of the ductility factor is closely linked to pushover analysis. Pushover analysis is a nonlinear static method that replicates the progressive plastic deformations of a structure subjected to increasing seismic loads. It provides a visual representation of a structure's behavior in terms of deformations. Consequently, evaluating the ductility factor often relies on observations and conclusions drawn from pushover curves to verify the structure's ability to withstand seismic loads.

4.1 Newmark and Hall method

The Newmark and Hall method is an earthquake analysis technique aimed at assessing the response of structures. Although it primarily focuses on seismic movements and the evaluation of deformations, accelerations, and displacements, it is not directly associated with the ductility of materials or structures. However, an analysis of seismic response using methods like Newmark and Hall can contribute to assessing ductility by providing data on how a structure deforms and withstands increasing seismic loads [13].

$$\begin{cases} R_\mu = \mu & \text{for } T > 0.5s \\ R_\mu = \sqrt{2\mu - 1} & \text{for } 0.2s \leq T \leq 0.5s \\ R_\mu = 1 & \text{for } T < 0.2s \end{cases}$$

T: Fundamental period of vibration of the structure.

4.2 Krawinkler and Nassar method

The Krawinkler and Nassar method is also based on the seismic response of a single-degree-of-freedom system with

Table 1 The values of the parameters (a and b) are given as a function of α

Post-elastic stiffness α in (%)	Parameters	
	A	b
0	1	0.42
2	1	0.37
10	0.8	0.29

elastoplastic behavior and hardening. The ductility factor is given by the following expression [14]:

$$R_\mu = [c(\mu - 1) + 1]^{1/c} \text{ With : } c(T, \alpha) = \frac{T^a}{1+T^a} + \frac{b}{T}$$

T: Fundamental period of vibration of the structure.

α : Post-elastic stiffness (%)

a and b : the values of these two parameters are located in Table 1.

4.3 Fajfar method

The ductility factor R_μ proposed by Fajfar in his N_2 method (N for nonlinear analysis and 2 for two mathematical models) takes into account the site-specific characteristic period and is expressed by the following relationship [15]:

$$\begin{cases} R_\mu = (\mu - 1) \frac{T}{T_c} + 1 & \text{for } T < T_c \\ R_\mu = \mu & \text{for } T \geq T_c \end{cases}$$

T Fundamental period of vibration of the structure.

T_C Characteristic period of the ground.

4.4 Priestley method

The ductility factor R_μ proposed by Priestley takes into account the site-specific characteristic period, and it is expressed by the following relationship [16]:

$$R_\mu = 1 + (\mu - 1) \frac{T}{1.5T_c}$$

T Fundamental period of vibration of the structure.

T_c Characteristic period of the ground.

5 Vulnerability assessment and identification of damage levels

When seismic shocks and subsequent structural responses are unclear, a structure's response is determined through a probabilistic seismic performance evaluation. The damage status of the building structure can be quantified in several ways, using the damage index [17, 18].

$$DI = \frac{\delta_m - \delta_y}{\delta_u - \delta_y}$$

δ_m Maximum inelastic displacement.

δ_u Ultimate displacement (total collapse).

δ_y Yield displacement.

Table 2 presents an equivalent between the previously defined damage index DI and the degradation state based on the degrees of structural damage.

If structural capacity and seismic demand are modeled by a lognormal distribution, the probability of reaching or exceeding a specific damage state also follows a lognormal distribution. This probability can be calculated using the lognormal cumulative probability density function, which is expressed as a cumulative function (Fig. 4) [18]. The lognormal cumulative probability density function is as follows:

$$P(S_d) = \Phi\left(\frac{1}{\beta_{ds}} \ln\left(\frac{S_d}{\bar{S}_{d,ds}}\right)\right)$$

where: $\bar{S}_{d,ds}$ is the median spectral displacement at which the structure crosses the damage state threshold ds, β_{ds} is the damage state ds standard deviation of the spectral displacement, and Φ is the distribution normal.

Table 2 Equivalence between damage index and damage status





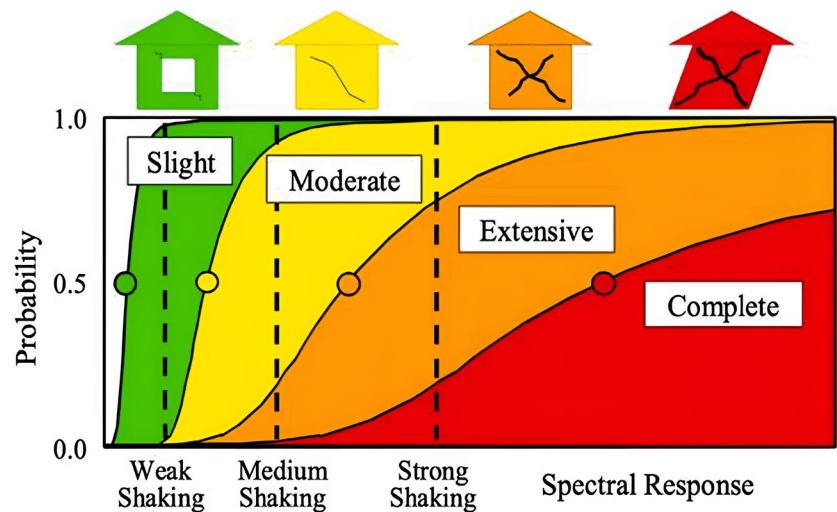
Degree of damage	Slight	Moderate	Extensive	Complete
Illustration				
Description	Non-structural hairline (diagonal or horizontal) cracks in infill walls; maybe crack sat the frame of an interface of infill wall	Severe damage of non-structural walls; extensive cracking in walls; maybe diagonal shear cracks in beams or columns	Partial or complete failure of the Structural component; out-of-plane bulging of infill walls; maybe permanent lateral deformation	Partial or total failure/collapse of the structure; total failure of infilled walls; non-ductile failure of columns and beams of concrete.
Damage index	0.1 < DI ≤ 0.25	0.25 < DI ≤ 0.4	0.4 < DI ≤ 1.0	DI > 1.0

Fig. 4 Levels of damage described by the fragility curves [18]



6 Description of the studied structures

6.1 Geometry

In our analysis, we will examine three reinforced concrete structures (Fig. 5). Each floor of these structures has a height of 3 m and is supported by reinforced concrete columns and beams (Table 3), ensuring an efficient distribution of vertical loads. As far as material characteristics are concerned, our choice of values is based on a combination of practical considerations and compliance with current design standards. The compressive strength of concrete, noted f_{ck} , was set at 25 MPa. This value was selected to reflect a strength

typical of concrete used in civil engineering structures, thus ensuring a certain robustness while remaining in line with current practice. The yield strength of steel reinforcement, noted F_e , was set at 400 MPa. This value is in line with quality standards for steels used in reinforced concrete structures. High yield strength steel reinforcement is essential to provide the necessary resistance to tensile loads in the structure, which is particularly important in seismic conditions [19]. The structures must be located in zones of increasing seismicity, namely: zones 3, 4, and 5, with zone acceleration coefficients of 0.1, 0.14, and 0.18. The seismic loads acting on the studied structures are lateral forces applied to the different levels of the system.

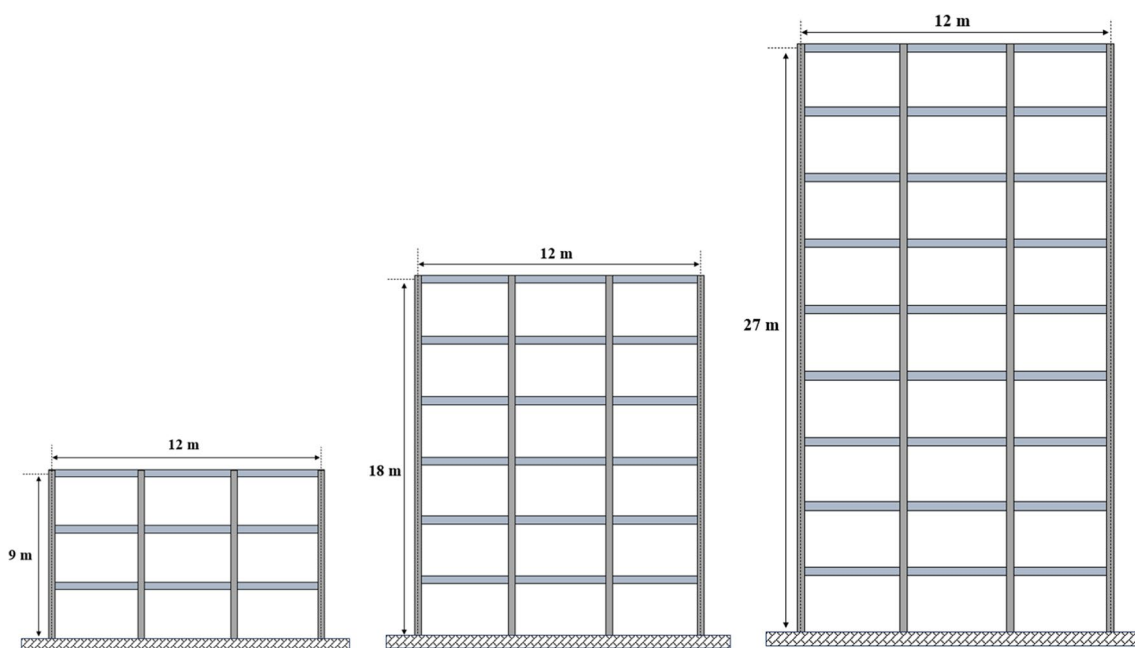
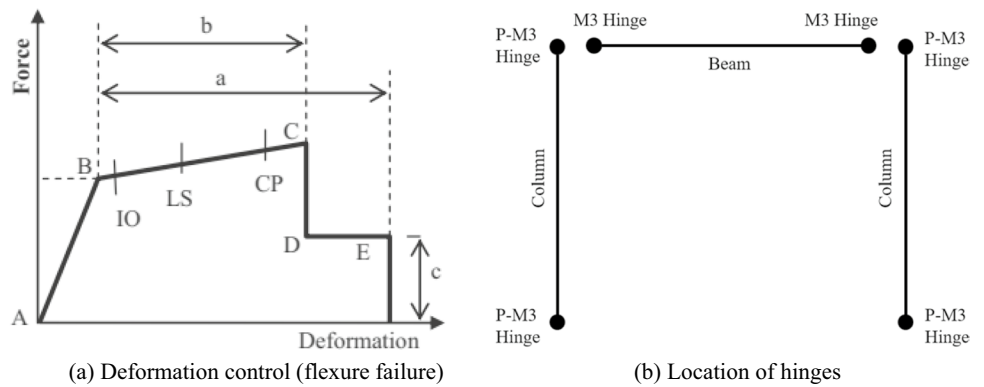


Fig. 5 General view of the 2D models

Table 3 Cross-sectional area and adopted steel rebar for structures with seismic code

Floor	Cross-sectional area (cm)		Steel rebar	
	Beam	Column	Beam	Column
3-story				
Floor 1–3	25 × 30	30 × 30	6T14	8T14
6-story				
Floor	Cross-sectional area		Steel rebar	
	Beam	Column	Beam	Column
Floor 1–3	30 × 30	30 × 35	6T14	8T14
Floor 4–6	25 × 30	30 × 30	4T14 + 2T12	4T14 + 2T12
9-story				
Floor	Cross-sectional area		Steel rebar	
	Beam	Column	Beam	Column
Floor 1–3	30 × 35	35 × 40	8T16	8T16
Floor 4–6	30 × 30	30 × 35	6T14	8T14
Floor 7–9	25 × 25	25 × 30	6T12	4T14 + 2T12

Fig. 6 Idealized inelastic force–deformation relationship [21]



Within this research, beam and column components were simulated as nonlinear frame elements. To model these, concentrated M3 and PM3 plastic hinges were attributed to

both ends, following the guidelines outlined in FEMA 356. Figures 6 and 7 display the acceptance criteria, denoted as IO, LS, and CP, for the ultimate rotation capacity [20, 21].

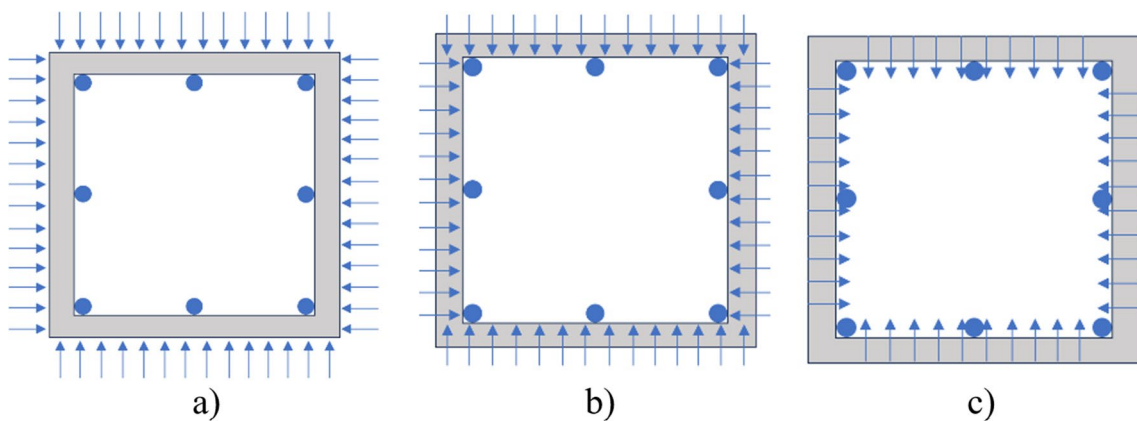


Fig. 7 Schematic representation of the application of seismic loads on a section's boundary at various performance levels. **a** IO level of performance. **b** LS level of performance. **c** CP level of performance [21]

Table 4 Seismic Data of each zone

Parameter	Zone 3	Zone 4	Zone 5
Soil factor S	1.2	1.2	1.2
Horizontal ground acceleration A	0.1	0.14	0.18
Behavior factor R	3,4	3,4	3,4

6.2 Seismic data

The integration of seismic data into SAP2000 software provides a comprehensive analysis and design of structures under seismic loads. This process involves incorporating seismic parameters into the software to accurately simulate the behavior of structures during seismic events (Table 4) [22].

7 Results

7.1 Capacity curves of the studied frames

The pushover method provides a clear visualization of a structure's load-bearing capacity and deformation in the event of an earthquake. It helps identify the most vulnerable

areas of the structure by pinpointing structural elements prone to excessive deformations or failures. This information is crucial for designing reinforcement strategies and assessing a structure's seismic resistance capacity.

The pushover curve is a structural analysis tool used to assess a structure's behavior under incremental lateral loads, simulating the effects of an earthquake. This curve illustrates the relationship between the applied lateral force and the overall displacement of the structure. It is obtained by gradually applying increasing horizontal loads at different levels of the structure until significant deformation levels are reached.

The Fig. 8 depicts pushover curves associated with each of the structure and for each seismic zone. It is evident from the analysis that the base shear force increases with higher seismic intensity, while conversely, this value decreases with increasing structure height.

7.2 Damage assessment of structures

For the computation of the introduced DIs, the collapse mechanism obtained from pushover analysis for different structures is used. Figure 9 depicts the plastic hinge formation in the 3-storey structure for each seismic excitation. The collapse mechanism is expected to help in identification

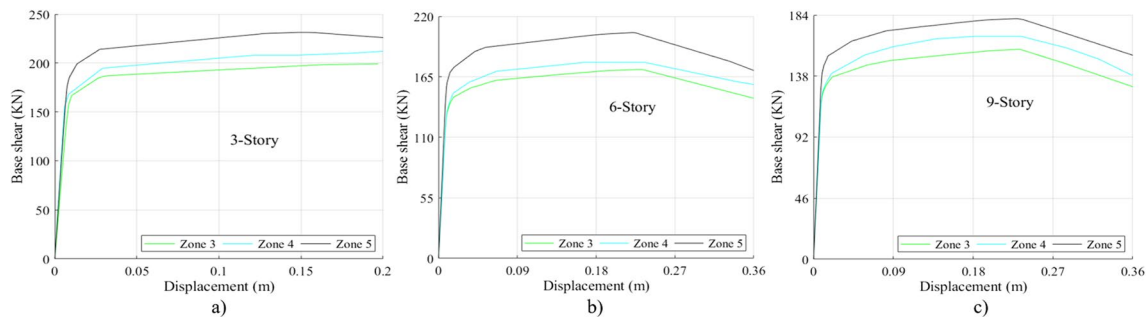


Fig. 8 Capacity curves for each structure: **a** 3-Story **(b)** 6-Story **(c)** 9-Story

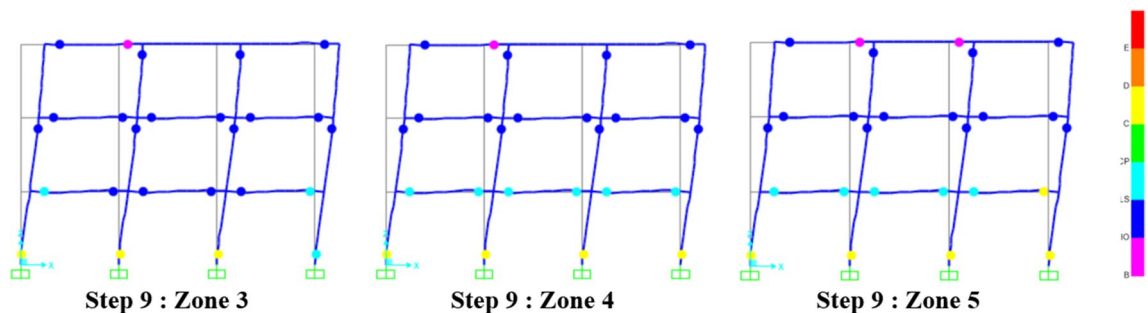


Fig. 9 Mechanism of plastic hinge formation of a 3-Story structure and for each zone

Table 5 Collapse mechanism of a 3-Story structure in Zone 3

Step no	Displ. (m)	Different performance levels							
		A-B	B-IO	IO-LS	LS-CP	CP-C	C-D	D-E	Total
1	0,007	40	2	0	0	0	0	0	42
6	0,027	20	22	0	0	0	0	0	42
7	0,063	20	15	7	0	0	0	0	42
8	0,099	17	2	19	4	0	0	0	42
9	0,127	17	1	18	3	0	3	0	42

of failure modes and the location of the weak points of the structure. The plastic hinge formation and transfer from one performance level to the other was analyzed to obtain various response parameters. According to Assumption (The appearance of the first hinge within the operational level is used as a measure of initial stiffness of the structure), the appearance of the first crack or hinge within the operational level is considered to be a measure of the initial stiffness or intact stiffness (which appears to be at Step 1 of pushover for all push load cases). Tables 5, 6, and 7 provide details of the collapse mechanism for a 3-story structure.

The studied damage variable is a displacement value at various performance levels. The threshold value of the damage variable is the maximum displacement at the operational level (at Step 6 for a 3-story structure and for each seismic zone). The minimal value of the damage variable is the displacement at collapse (at Step 9 for a 3-story structure and for each seismic zone). The other observed values of the damage variable correspond to the displacement at different performance levels (at Steps 7, and 8 for a 3-story structure and for each seismic zone). The calculated values of DI at various performance levels are illustrated in Table 8.

The collapse mechanism, derived from pushover analysis for various structures, is presented in Table 9. Furthermore, based on the calculation of the damage index, it is observed that the value of the damage index (DI) increases with the increase in the seismicity of the area and the height of the structure under study.

It is essential to emphasize that structures of lesser height pose a lower risk of collapse compared to medium and large-scale structures. This observation stems from several factors. Firstly, structures of lesser height are subjected to lower seismic forces due to their lower total mass. Additionally, their center of gravity is typically closer to the ground, reducing torsion moments and leverage effects in the event of an earthquake.

Conversely, medium and large-scale structures are more prone to accumulating significant damage due to their greater height and larger mass. They are more susceptible to torsion and shear effects induced by seismic forces, increasing their vulnerability to collapse.

Therefore, the height of the structure plays a crucial role in its risk of collapse during an earthquake, and it is essential to consider this factor in the design and evaluation of buildings to ensure their safety and resilience to earthquakes.

Table 6 Collapse mechanism of a 3-Story structure in Zone 4

Step no	Displ. (m)	Different performance levels							
		A-B	B-IO	IO-LS	LS-CP	CP-C	C-D	D-E	Total
1	0,007	40	2	0	0	0	0	0	42
6	0,029	18	24	0	0	0	0	0	42
7	0,067	18	15	9	0	0	0	0	42
8	0,121	17	2	21	2	0	0	0	42
9	0,143	17	1	14	6	0	4	0	42

Table 7 Collapse mechanism of a 3-Story structure in Zone 5

Step no	Displ. (m)	Different performance levels							
		A-B	B-IO	IO-LS	LS-CP	CP-C	C-D	D-E	Total
1	0,007	40	2	0	0	0	0	0	42
6	0,032	18	24	0	0	0	0	0	42
7	0,089	17	12	12	0	0	0	0	42
8	0,158	17	2	18	5	0	0	0	42
9	0,163	16	2	14	5	0	5	0	42

Table 8 Plastic-ductility damage indices of a 3-Story

Performance levels	Zone 3			Zone 4			Zone 5		
	Step no	d (m)	DI	Step no	d (m)	DI	Step no	d (m)	DI
A-B	1	0,007	-	1	0,007	-	1	0,007	-
IO	6	0,027	0.1	6	0,029	0.11	6	0,032	0.13
LS	7	0,063	0.29	7	0,067	0.31	7	0,089	0.42
CP	8	0,099	0.48	8	0,121	0.59	8	0,158	0.78
C	9	0,127	0.63	9	0,143	0.7	9	0,163	0.8
Ultimate displacement	0.196			0.2				0.2	

7.3 Behavior factor R of the studied structures

In the present study, the behavior factor R of the studied system is evaluated by taking into account the reduction factor Ω due to the overstrength of the structure as well as its deformation capacity in the plastic domain: reduction factor R_{μ} due to its overall ductility.

$$R = R_{\mu} \Omega$$

With:

R_{μ} Reduction factor due to the ductility of the structure.

Ω Reduction factor due to the overstrength of the structure.

It is very useful to conduct a comparative study of the R values evaluated for different structures and in different regions (zones 3, 4, and 5) of Morocco. Table 10 and Fig. 10 show that this value ($R=3.4$) is only valid for low-rise structures and decreases with the elevation of the structure. It is therefore important to note that the behavior factor varies contrary to what is observed in most seismic construction standards.

7.4 Fragility curves

Fragility curves, developed through the non-linear static method, offer a visual depiction of potential structural damage or failure levels in response to seismic excitation. Typically, these curves illustrate the probability of failure relative to spectral displacement.

Probability, in terms of seismic risk assessment with the Hazus tool, is intimately linked to the intrinsic characteristics of structures. Hazus classifies structures according to three fundamental parameters: structural system, design code, and building height. These elements form the basis of building typology and are essential for assessing the probability of seismic damage.

The structures examined in this study were identified as C1L-HC (3-story), C1M-HC (6-story), and C1H-HC (9-story) type structures due to the following factors (Table 11):

7.4.1 Reinforced concrete structural system (C1)

The structure is in reinforced concrete, which in accordance with the Hazus classification, categorizes it as a C1-type structure. This classification is determined on the basis of the material's mechanical properties and resistance characteristics.

Table 9 Plastic-ductility damage indices for each structure

Structures	Damage index (DI)											
	Zone 3				Zone 4				Zone 5			
	IO	LS	CP	C	IO	LS	CP	C	IO	LS	CP	C
3-Story	0.1	0.29	0.48	0.63	0.11	0.31	0.59	0.7	0.13	0.42	0.78	0.8
6-Story	0.16	0.32	0.51	0.73	0.18	0.38	0.64	0.76	0.22	0.49	0.82	0.88
9-Story	0.23	0.39	0.58	0.81	0.28	0.45	0.72	0.88	0.31	0.53	0.88	0.94

Table 10 Summary of the values of R_μ , R_μ^* (The average value of R), Ω and R for the different structures

Structures	Method	Zone 3				Zone 4				Zone 5			
		R_μ	R_μ^*	Ω	R	R_μ	R_μ^*	Ω	R	R_μ	R_μ^*	Ω	R
3-Story	Newmark and Hall	1.97	2.01	1.6	3.2	2.03	2.1	1.66	3.48	2.1	2.2	1.7	3.74
	Krawinkler and Nassar	2.1				2.2				2.3			
	Fajfar	2.06				2.1				2.24			
	Priestley	1.9				1.98				2.08			
6-Story	Newmark and Hall	2.12	2.2	1.2	2.64	2.18	2.25	1.26	2.84	2.24	2.28	1.3	2.96
	Krawinkler and Nassar	2.31				2.38				2.4			
	Fajfar	2.24				2.3				2.32			
	Priestley	2.1				2.14				2.18			
9-Story	Newmark and Hall	2.18	2.2	1.04	2.28	2.2	2.27	1.1	2.48	2.26	2.32	1.14	2.64
	Krawinkler and Nassar	2.41				2.4				2.42			
	Fajfar	2.28				2.32				2.38			
	Priestley	2.12				2.16				2.22			

7.4.2 Design code RPS2000, classified HC (high code)

The structure design complies with RPS2000, a specific design code. According to Hazus, RPS2000 is classified as High Code (HC), indicating a high level of structural rigidity and strength in line with rigorous design standards.

7.4.3 Height and number of floors (L (Low) /M (Middle) /H (High))

The structures are 3, 6, and 9 stories.

The vulnerability curves of a structure relate a spectral parameter to the probability. We can induce from the figures that each fragility curve represents a damaged state. We have chosen to represent the fragility curves as a function of the spectral displacement in each region (Fig. 11).

7.5 Probability of collapse of structures in different seismic zones

The vulnerability curves of a structure are used primarily to assess the seismic risk of structures, and through a simple

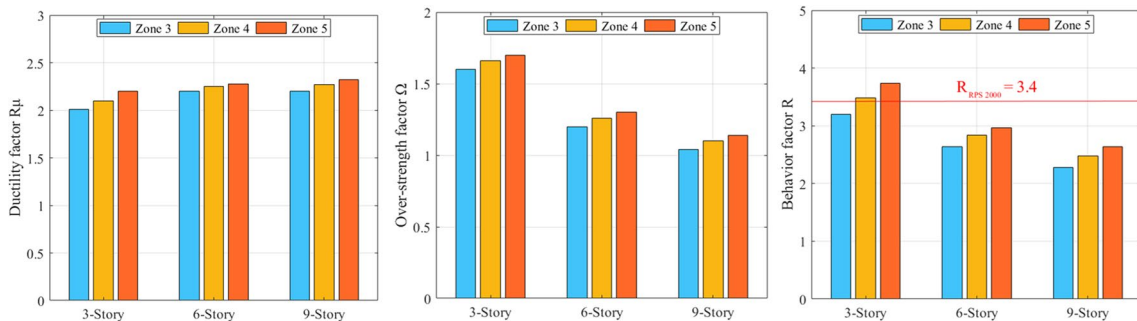


Fig. 10 Behavior factors for the structures studied

Table 11 Hazus parameters for reinforced concrete structures

Structures	Slight		Moderate		Extensive		Complete	
	$\bar{S}_{d,ds}$ (cm)	β_{ds} (-)	$\bar{S}_{d,ds}$ (cm)	β_{ds} (-)	$\bar{S}_{d,ds}$ (cm)	β_{ds} (-)	$\bar{S}_{d,ds}$ (cm)	β_{ds} (-)
3-Story (C1L-HC)	2.29	0.81	4.58	0.84	13.72	0.86	36.58	0.81
6-Story (C1M-HC)	3.81	0.68	7.6	0.67	22.9	0.68	61	0.81
9-Story (C1H-HC)	5.48	0.66	10.97	0.64	32.92	0.67	87.8	0.78

probability, calculation can determine the risk associated with each seismic zone.

In this section, the evaluation of the target displacement, also referred to as the performance point, will be carried out in accordance with Eurocode 8. This evaluation focuses exclusively on the contribution of the fundamental vibration mode, using the load capacity defined by Eurocode 8. Capacity curves are generated from a

uniform lateral load model. The methodology adopted is based on the superposition of two significant curves. The first represents the capacity of the structure, derived from a non-linear static analysis (pushover). The second represents the earthquake-induced stress, expressed as an inelastic response spectrum. The intersection of these two curves, representing respectively the capacity and the seismic demand, is then converted into the format of the

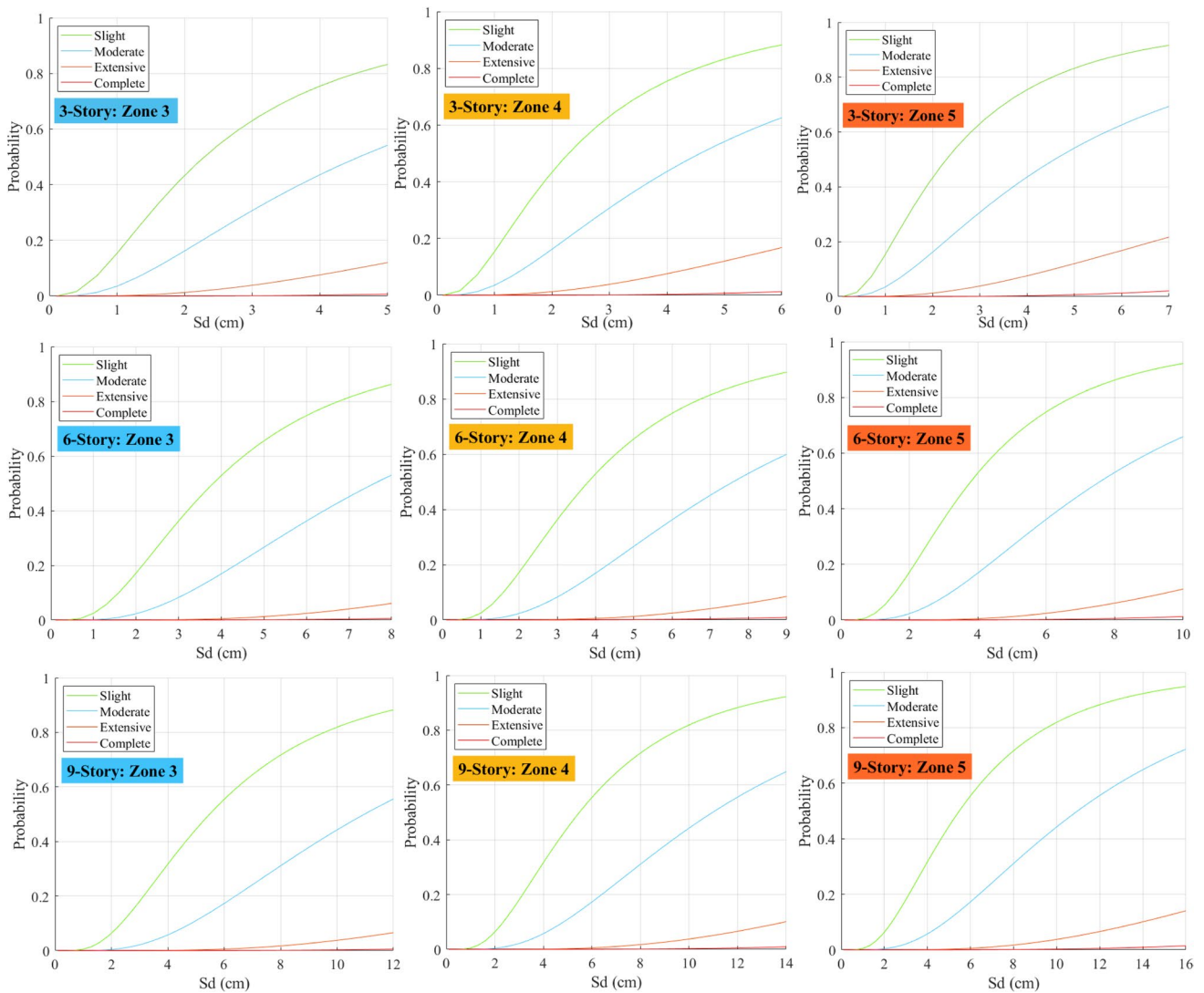


Fig. 11 Fragility curves of the structures in the different seismic zones

Table 12 Spectral displacement at performance point for structures located in different seismic zones

Structures	Spectral displacement at Performance Point (ATC 40) (cm)		
	Zone 3	Zone 4	Zone 5
3-Story	2.2	2.5	2.7
6-Story	4.2	4.5	4.8
9-Story	6.9	7.2	7.5

acceleration-displacement response spectrum (S_a-S_d), thus allowing to obtain the performance point (Table 12).

Using the data from Table 12 regarding spectral displacement at the performance point level, we can deepen our analysis and draw meaningful conclusions regarding the risk probability presented in Table 13 and Fig. 12. These data enable us to establish connections between spectral displacement levels and the associated risk levels at each level of the structure in different seismic zones.

By examining Table 13 and Fig. 12, we can identify trends and variations in risk probability across different levels of the structure and different seismic zones. For instance, we can observe how the risk probability evolves with increasing spectral displacement in each seismic zone, or how it differs from one zone to another based on the specific seismic characteristics of each region.

These visualizations provide a comprehensive perspective on how seismic risks are distributed across the structure and regions, which is crucial for accurate risk assessment and the implementation of effective mitigation measures. By better understanding the relationship between spectral displacement levels and risk levels, design and engineering professionals can make informed decisions to enhance the seismic resilience of structures and reduce the potential impacts of earthquakes.

8 Discussion

Most seismic codes maintain the factor R constant, regardless of the height of the structure under consideration. However, this stability is primarily observed in low-rise structures. To assess this influence, we examined the behavior factor R of structures with 3, 6, and 9 stories located in different seismic zones, following the Moroccan regulations (RPS 2000). Additionally, the behavior factor R , which combines ductility (R_μ) and resistance (Ω) reductions, increases with increasing seismic intensity. This increase in R is more closely associated with variations in the resistance factor than with those in the ductility factor.

The results highlight two important points regarding the impact of height and seismicity of the area on the behavior factor. Firstly, the value of R increases with the intensification of the seismic zone, revealing a deficiency in the standard that assumes all three zones have the same value of behavior factor R . Secondly, this value decreases with the elevation of the structure's height. For zone 3, the average value of the structure's R factor is 3.2 for a 3-story structure, in accordance with seismic regulations. However, with increasing height, there is a decrease in this factor, which questions another deficiency in the standard that maintains this value constant regardless of the number of stories in the studied structure.

In addition to that, we aim to integrate the probabilistic method into seismic construction codes, which involves adopting a more dynamic and evolving approach to assess seismic risks. This would involve considering the inherent variability in seismic phenomena rather than relying solely on fixed values or simplified models. Incorporating this probabilistic method into seismic regulations could provide a more accurate understanding of risks, leading to more suitable construction standards and better seismic preparedness.

Table 13 Probability of risk for structures located in different seismic zones

Structures	Zone 3				Zone 4				Zone 5			
	Slight	Moderate	Extensive	Complete	Slight	Moderate	Extensive	Complete	Slight	Moderate	Extensive	Complete
3-Story	0.48	0.19	0.002	0	0.54	0.23	0.002	0	0.58	0.26	0.002	0
6-Story	0.56	0.19	0.006	0	0.6	0.22	0.008	0	0.63	0.24	0.01	0
9-Story	0.64	0.23	0.01	0	0.66	0.25	0.011	0	0.68	0.28	0.013	0

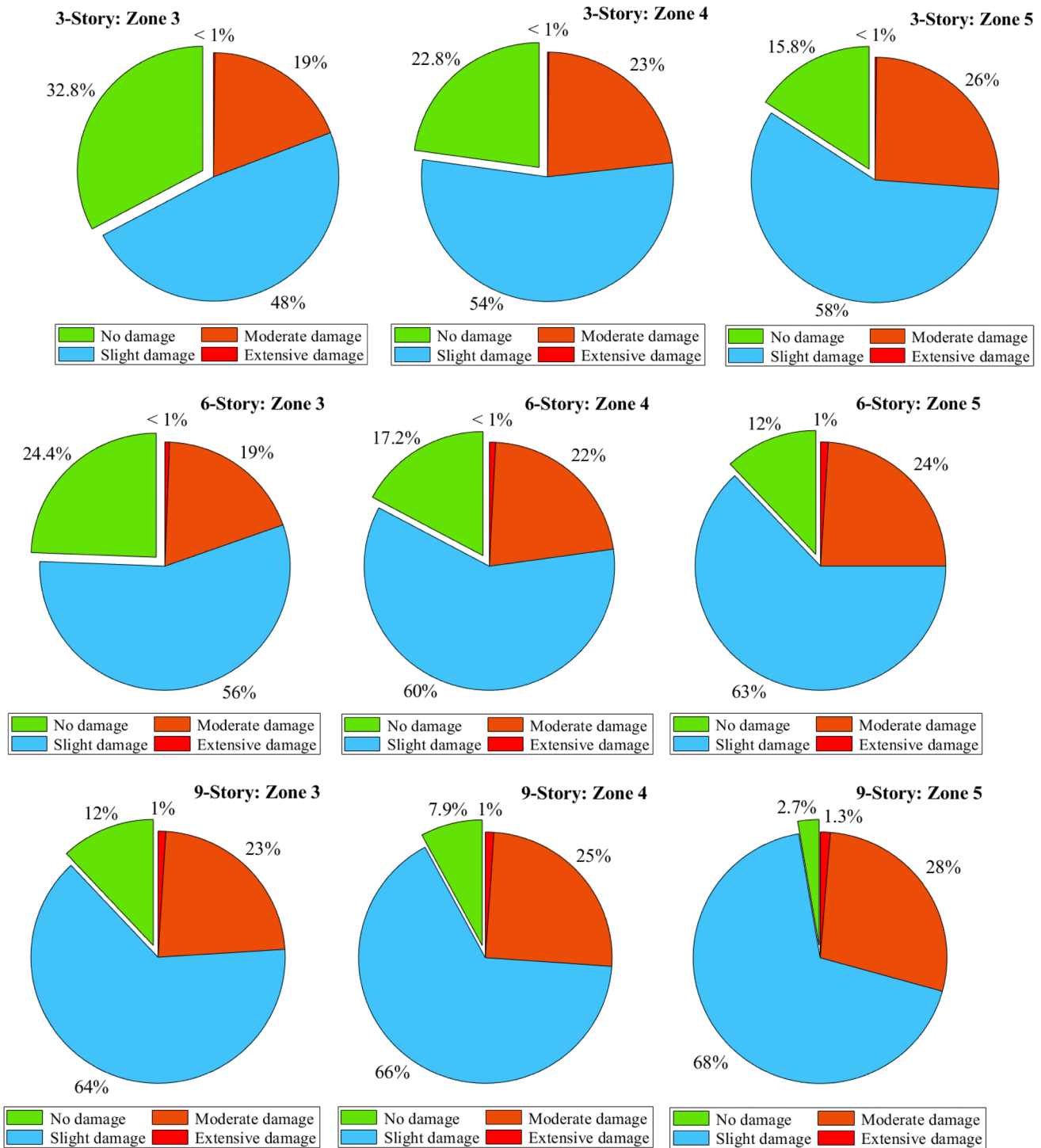


Fig. 12 Probability of risk for structures in different seismic zones

9 Conclusion

The aim of this article is to explore the impact of the zone (zones 3, 4, and 5) and the height of the structure on the value of the behavior factor R. In summary:

- The value of the behavior factor increases with the intensification of seismic activity.
- The value of the behavior factor decreases with the increase in the height of the structure.
- The factor R is primarily influenced by the variation in the over-strength factor rather than ductility. Thus, the

use of a single standardized value of this factor by most regulatory codes, regardless of the zone or height considered, appears unjustified.

The results of the pushover analysis, combined with fragility curves, allow for the assessment of the seismic vulnerability of structures and the quantification of damage probability in the event of an earthquake, providing crucial information on the resilience of structures. Fundamentally, our objective is to integrate the probabilistic method into the seismic construction regulation RPS 2000.

Author contributions Adil Ziraoui: Methodology, Investigation, Resources, Writing – original draft, Writing – review & editing. Benaissa Kissi: Conceptualization, Formal analysis, Writing – original draft, Writing – review & editing. Hassan Aaya: Validation, Formal analysis, Writing – original draft, Visualization. Najoua Mrabet: Conceptualization, Formal analysis, Writing – original draft, Writing – review & editing. Ilhame Azdine: Conceptualization, Software, Validation, Resources, Writing – original draft, Supervision.

Funding The authors declare that no funds, grants, or other support were received during the preparation of this manuscript.

Data availability No datasets were generated or analysed during the current study.

Declarations

Competing interests The authors declare no competing interests.

References

- Cherkaoui TE, Hatzfeld D, Jebli H, Medinan F, Caillot V (1990) Etude microsismique de la région d'Al Hoceima. *Bull Inct Sci Rabat* 12:25–34
- D'Ayala D, Speranza E (2003) Definition of collapse mechanisms and seismic vulnerability of historic masonry buildings. *Earthq Spectra* 19(3):479–509. <https://doi.org/10.1193/1.1599896>
- Yeck WL, Hatem AE, Goldberg DE, Barnhart WD, Jobe JAT, Shelly DR, Villaseñor A, Benz HM, Earle PS (2023) Rapid source characterization of the 2023 Mw 6.8 Al Haouz, Morocco. *Earthquake Seism Rec* 3:357–366. <https://doi.org/10.1785/0320230040>
- Bufoñ E, Galdeano CSD, Udias A (2004) Seismotectonics of the Ibero-Maghrebian region. *Tectonophysics* 30(248):247–261
- RPS. Règlement de Construction Parasismique. Ministère de l'Aménagement du Territoire, de l'Urbanisme, de l'Habitat et de l'Environnement; Secrétariat d'Etat à l'Habitat, Rabat, Morocco 17
- RPS (2000) Règlement de Construction Parasismique, Version 2011, Ministère de l'Habitat, de l'Urbanisme et de l'Aménagement de l'Es-pace, Rabat, Morocco
- Kassem MM, Mohamed Nazri F, Norooznejad Farsangi E (2020) The seismic vulnerability assessment methodologies: a state-of-the-art review. *Ain Shams Eng J* 11:849–864. <https://doi.org/10.1016/j.asej.2020.04.001>
- Applied Technology Council, ATC-40 (1996) Seismic evaluation and retrofit of concrete buildings, California 1 and 2
- Kim S, D'Amore E (1999) Pushover analysis procedure in earthquake engineering. *Earthq Spectra* 15:417–423. <https://doi.org/10.1193/1.1586051>
- Ziraoui A, Kissi B, Aaya H, Azdine I (2023) Techno-economic study of seismic vulnerability in reinforced concrete structures by composite materials. *Int Rev Civ Eng IRECE* 14:561. <https://doi.org/10.15866/irece.v14i6.22940>
- Ziraoui A, Kissi B, Aaya H, Mezriahi Y, Haimoud A (2023) Seismic retrofitting: analyzing the effectiveness of RC shear walls and CFRP reinforcement for RC structures. pp 203–214. https://doi.org/10.1007/978-3-031-49345-4_21
- Elnashai AS (2001) Advanced inelastic (pushover) analysis for earthquake applications. *Struct Eng Mech* 12:51–6. <https://doi.org/10.12989/sem.2001.12.1.051>
- Newmark NM, Hall WJ (1982) Earthquake spectra and design. EERI Monograph Series, EERI, Oakland, CA, USA
- Krawinkler H, Nassar AA (1992) Seismic design based on ductility and cumulative damage demand and capacities. In: Fajfar P, Krawinkler H (eds) *Nonlinear seismic analysis and design of reinforced concrete buildings*. Elsevier applied science, New York
- Fajfar P (2002) Structural analysis in earthquake engineering a breakthrough of simplified nonlinear methods. 12th European conference on earthquake engineering
- Mander JB, Priestley MJN (1988) Observed stress-strain behavior of confined concrete. *J Struct Eng ASCE* 114(8):1827–1849
- Shome N, Cornell CA (1999) Probabilistic seismic demand analysis of nonlinear structures. Tech. Rep. RMS–35, RMS Program, Stanford University, CA
- FEMA (1999) “HAZUS Earthquake loss estimation methodology”, Federal emergency management agency, Washington, D.C.
- BAEL 91. Règles techniques de conception et de calcul des ouvrages et constructions en Béton Armé suivant la Méthode des Etats limites. Edition Eyrolles: 1992, Paris, France. ISBN: 221210023X
- Tbatou T, El Youbi M (2020) Dynamic and structural study of a RC building braced by FRP composite materials. *Int Rev Civil Eng* 11(1):1–9. <https://doi.org/10.15866/irece.v11i1.16991>
- Ziraoui A, Kissi B, Aaya H (2024) Probabilistic analysis of FRP efficacy in seismic risk reduction. *Forces Mech* 100259. <https://doi.org/10.1016/j.finmec.2024.100259>
- (2005) CSI Analysis Reference Manual for SAP2000, ETABS, and SAFE – computers and structures, Inc. Berkeley, California, USA

Publisher's Note Springer Nature remains neutral with regard to jurisdictional claims in published maps and institutional affiliations.

Springer Nature or its licensor (e.g. a society or other partner) holds exclusive rights to this article under a publishing agreement with the author(s) or other rightsholder(s); author self-archiving of the accepted manuscript version of this article is solely governed by the terms of such publishing agreement and applicable law.